Discharge of the Nanopore Confinement Effect on the Glass Transition Dynamics via Viscous Flow

K. Adrjanowicz* and M. Paluch
Institute of Physics, University of Silesia, Ulica 75 Pulku Piechoty 1, 41-500 Chorzow, Poland and Silesian Center for Education and Interdisciplinary Research (SMCEBI), Ulica 75 Pulku Piechoty 1a, 41-500 Chorzow, Poland

(Received 20 October 2018; published 3 May 2019)

Using dielectric spectroscopy, we demonstrate that confinement-induced changes in the glass transition dynamics, as observed for polymethylphenylsiloxane in alumina nanopores, reveal a pronounced nonequilibrium nature. Our results indicate that glass formers confined to nanopores are able to recover their bulklike mobility. We found that the characteristic time constant of such an equilibration process correlates with an extremely slow viscous flow rate in cylindrical channels of nanometer size. Thus, all the way to equilibrium, confinement effects seen in faster segmental dynamics are released through the viscous flow which eventually helps to eliminate surplus volume gained by nanoconstrained polymers upon cooling.

DOI: 10.1103/PhysRevLett.122.176101

One of the most prominent and widespread manifestations of the 2D confinement effect on the glassy dynamics is a deviation of the temperature dependence of the α-relaxation time from the Vogel-Fulcher-Tamman (VFT)-behavior characteristic for a bulk material [1,2]. Over the past decade, this appealing finding was related to various concepts, e.g., dynamic exchange process or approaching the limit of cooperativity correlation length [3–5]. However, recent studies provide strong experimental evidence that a kink in the $\tau_\alpha(T)$ dependence observed for a large class of glass formers confined in nanopores corresponds to vitrification of the interfacial layer at $T_{g\_\text{interface}}$ [6–9]. Below that temperature, a kinetic arrest of the interfacial layer on the time scale of the experiment leads to frustration in the density of the nanoconfined system that favors quasi-isochoric (constant volume) conditions. Provided that the α relaxation is fairly sensitive to volume effects, this results in faster dynamics as compared to the bulk.

Since vitrification of the interfacial layer at $T_{g\_\text{interface}}$ possesses all the characteristic features of the glass transition event [7,10,11], we might expect that confined material enters an out-of-equilibrium regime below that temperature. Therefore, similar to bulk glasses kept below T_g, it should spontaneously evolve ("age") towards an equilibrium state and try to increase its density frozen at $T_{g\_\text{interface}}$. This way of thinking is actually supported by experimental results showing that the glass transition behavior in nanopores, as well as the evolution of $\tau_\alpha(T)$ measured below $T_{g\_\text{interface}}$, varies depending on the cooling rate or annealing time [8,12–15]. However, it is not clear what drives the kinetics of such an equilibration process and what the equilibrium level is that glass-forming liquids and polymers confined to nanopores want (or are able) to reach.

In general, nontrivial features in physical aging of glasses are intrinsically challenging [16,17]. When spatially restricted at the nanoscale, additional contributing factors appear, such as preparation methods, processing history, or surface effects [18–20]. As anticipated by Simon and coworkers based on enthalpy recovery data for the molecular glass-former orthoterphenyl confined in controlled pore glass (CPG), the equilibrium state reached for the constrained material must be different from that of the bulk [21]. On the other hand, recent studies on thin polymer films demonstrate that it is possible to regain the bulklike dynamics in 1D confinement when providing enough time for the polymer chains located in close proximity of the supporting substrate to rearrange and attain more dense packing [22–24].

In this Letter, we aim to shed some light on the nonequilibrium glass transition dynamics restricted in two dimensions by cylindrical nanopores. We find that confinement effects—seen as faster α relaxation—weaken with time, and eventually, the system recovers bulklike mobility. The kinetics of such an equilibration process was investigated as a function of temperature and pore diameter. We identify that the equilibration mechanism in 2D hard confinement is related to the exceedingly slow magnitude of the viscous flow in cylindrical channels of nanometer size. The results suggest that the enhanced dynamics of the nanopore-confined system is only a matter of flow time needed to eliminate surplus volume gained upon cooling at $T_{g\_\text{interface}}$.

The sample tested is poly(phenylmethylsiloxane), with $M_n = 21.7k$ and polydispersity 1.28, acquired from Polymer Source (Canada). The choice of the siloxane-based polymer for this type of study is not accidental. In comparison to other polymers, PMPS shows a pronounced influence of the pressure or volume effects on the dynamics, which can be

related to a large degree of flexibility of the siloxane backbone [25–28]. Since volume plays an important role in the supercooled dynamics of PMPS, it is more likely that, in restricted geometry, this material shows significant deviation from the bulklike behavior, as also reported in the literature [29–32]. Therefore, PMPS was chosen as a model polymer glass former to investigate various aspects related to out-of-equilibrium dynamics in nanopore confinement. As confining matrices, we use commercially available anodized aluminum oxide (AAO) membranes characterized by uniform arrays of unidirectional and non-cross-linked cylindrical channels (from 10 to 200 nm in diameter and 100 μm in length) of strong hydrophilic character of the inner walls. The interactions of the surface polymer molecules with alumina walls can be parametrized via an interfacial energy, as demonstrated by Alexandris and coworkers [33]. According to literature data [34,35], the radius of gyration of the tested polymer is rather small (~0.7 nm; for comparison polystyrene ~2.5 nm), meaning that when confined in AAO membranes of pore diameters from 100 to 20 nm, we are still far above the relevant range of molecular dimensions. Changes in the α-relaxation dynamics in the presence of 2D-geometrical restrictions were investigated, either as a function of temperature or time, by using dielectric spectroscopy. More details on materials and methods can be found in the Supplemental Material (SM) [36].

In Figure 1, we have plotted the temperature dependence of the segmental (α)-relaxation time for PMPS in the bulk and inside 100 nm-diameter AAO templates. The relaxation time was estimated from the frequency at the maximum peak position, $\tau_\alpha = 1/(2\pi f_{\max})$. For nanopore confined material, we use two thermal protocols (i) slow cooling with the rate of ~0.2 K/ min and (ii) cooling jumps, with 5 K/ min, starting at room temperature down to six different temperatures between 260.5 and 248 K. The results demonstrate that, depending on the chosen protocol, evolution of $\tau_\alpha(T)$ in nanopores might look a bit different (additional data can be found in [36]). As can be seen in Fig. 1, results for $\tau_\alpha(T)$ obtained below $T_{g\_\text{interface}}$ can be described via isochores. In order to generate isochores, a combination of pressure-volume-temperature (PVT) and high-pressure dielectric relaxation measurements is required for a bulk material. From the first one, we obtain changes in the specific volume as a function of temperature and pressure, while the second one yields the behavior of the α-relaxation time at different combinations of T and p. By parametrization of the PVT data with the use of the Tait equation of state [39], we can convert from experimentally measured $\tau_\alpha(T,p)$ to $\tau_\alpha(T,V)$ dependences. To describe the evolution of the α-relaxation time in the entire T-V space, we have applied the modified version of the Avramov model [40]. With that, we can generate the isochoric dependences and use them to describe α-relaxation times in either the positive (bulk high-pressure) or negative pressure regime (nanopores), see

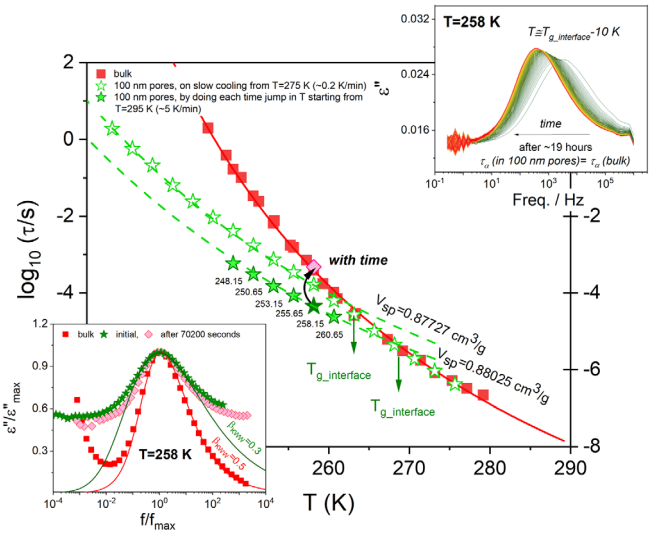

FIG. 1. Segmental (α-) relaxation time plotted vs temperature for PMPS in the bulk and confined to 100 nm AAO nanopores as measured using different thermal protocols. Evolution of the α-relaxation times measured in the temperature region when confined dynamics start to deviate from the bulk was described using two different isochoric dependences—extracted from PVT and high-pressure data for bulk PMPS. The upper inset shows changes in the α-loss peak position for confined to 100 nm pores PMPS at 258 K (i.e., roughly 10 K below $T_{g\_\text{interface}}$ of the quenched sample). The lower inset shows a comparison of the normalized dielectric loss spectra for bulk PMPS and confined to 100 nm nanopores as recorded before and after prolonged annealing at 258 K.

SM for more details [36]. More importantly, this approach is expected to apply for all glass-forming systems which obey the density scaling.

Note that, when approached with faster cooling rates, the surplus volume available in confinement will always be higher. Relative to the bulk case, the increase of the specific volume for a nanopore-confined polymer can be related to an increase in the free volume (more space available for molecules to move) [41]. This effect has also been seen in positron annihilation lifetime spectroscopy experiments [29,42].

Knowing that the dynamics of nanopore-confined PMPS shows a pronounced nonequilibrium behavior below $T_{g\_\text{interface}}$, we have carried out a prolonged-time dependent study (covering ~2 days) to characterize it in more detail. In the following, this will be referred to as an annealing experiment. We have started with samples confined to 100 nm pores annealed at different temperatures. All measurements were performed by following the same thermal treatment protocol, i.e., cooling with the rate of 5 K/ min from 295 K to a desired annealing temperature, T_{ANN}. The upper inset in Fig. 1 illustrates representative changes in the dielectric loss spectra recorded with time. We observe that the peak maximum moves systematically towards lower frequencies, indicating that the segmental dynamics, initially faster in confinement, slows down as

time passes. After ~19 hours of annealing at 258 K, such an equilibration process was completed, allowing the system in 100 nm pores to regain the α-relaxation time characteristic of the bulk polymer (see pink diamond symbols in Fig. 1). By analyzing changes of τ_α as a function of time, we can obtain valuable information about the kinetics. Interestingly, even at the very final stages of the annealing process, when the averaged relaxation time matches the bulk value, the segmental dynamics still reveals strongly heterogeneous behavior. As illustrated in the lower inset of Fig. 1, the distribution of the α-relaxation time narrows with annealing time, but eventually couldn't reach that of the macroscopic sample. Qualitatively, the same scenario applies to PMPS confined to 100 nm pores and annealed at other temperatures. However, with increasing the depth of annealing (the distance from $T_{g\_\text{interface}}$), the time needed to reach an equilibrium state exceeds experimentally accessible time frames. To describe the equilibration kinetics, a variation of the α-relaxation time during annealing was parametrized with the use of the stretched exponential function, as demonstrated in SM [see Fig. S7(a) [36]].

Except narrowing the dielectric loss spectrum and its shift towards lower frequencies, the intensity of the α relaxation increases with annealing time, see the upper inset in Fig. 1. We envision that this effect comes from the dipolar species which initially were immobilized by the interactions with the confining pore walls, but as the equilibration proceeds, they start to contribute to the α-relaxation dynamics. For PMPS embedded in 100 nm pores, $\Delta\epsilon$ increases by approx. 10%–15%. Interestingly, this value coincides with the thickness of the interfacial layer, $\xi \approx 15$ nm in 100 nm, as estimated based on calorimetric data (see results and additional discussion in SM) [6,36,43,44].

Nonequilibrium behavior in 2D-restricted geometry was also observed upon isothermal annealing of PMPS in AAO nanopores of different pore sizes (from 200 to 10 nm). At $T_{\text{ANN}} = 258$ K, likewise, τ_α increases with time and approaches that of the macroscopic sample (see Fig. S8 [36]). When embedded within relatively large pores, a nanopore-confined polymer easily recovers its bulk α-relaxation time characteristic for a given temperature. However, as the pores become smaller, confinement effects seen in faster dynamics are only partially wiped out after two days of annealing (see Fig. S8, solid symbols).

To analyze the departure from equilibrium bulklike dynamics we plot together $\log_{10}(\tau_{\text{bulk}})$ and $\log_{10}(\tau_{\text{confined}})$ recorded at the initial and final stages of the annealing process. The results originating from temperature and pore size-controlled experiments are presented as a function of the reduced temperature, defined as $\Delta T = T_{g\_\text{interface}} - T_{\text{ANN}}$, in Figs. 2(a) and 2(b), respectively. In both cases, when increasing the distance from $T_{g\_\text{interface}}$—the temperature at which perturbation in volume shows up—longer waiting times are needed to regain the mobility of the bulk material.

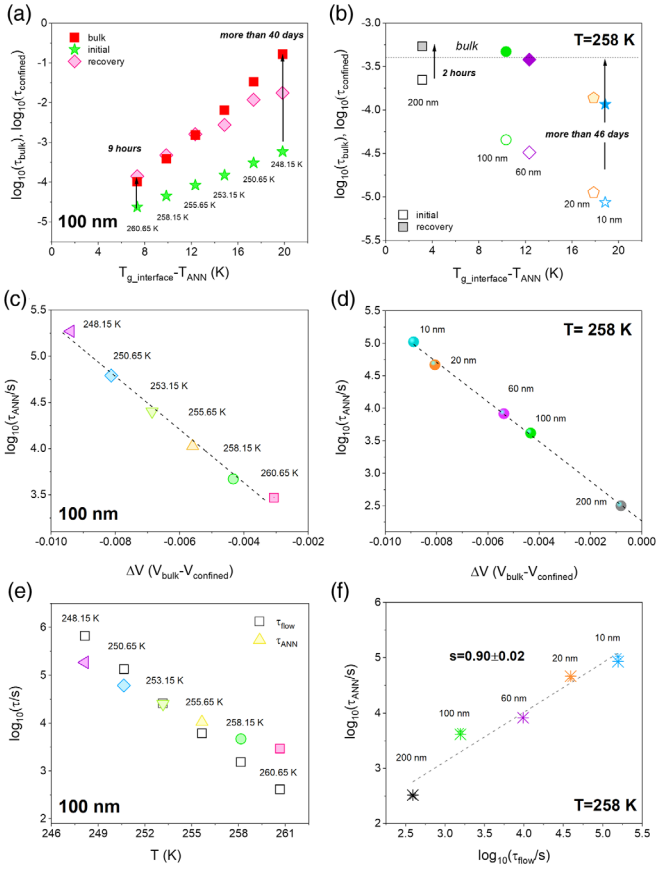

FIG. 2. Segmental relaxation times $\log_{10}(\tau_{\text{bulk}})$ and $\log_{10}(\tau_{\text{confined}})$ plotted vs the depth of the annealing upon temperature- (a) and size- (b) dependent studies. The dashed horizontal line indicates the bulk value of the segmental time, τ_{bulk}. The relationship between τ_{ANN} and $\Delta V = V_{\text{bulk}} - V_{\text{confined}}$ as obtained for the investigated polymer cooled with the rate of 5 K/ min from the room temperature down to sub-$T_{g\_\text{interface}}$ region and annealed therein (c) at few different temperatures in 100 nm pores and (d) under isothermal conditions in pores of the mean diameter ranging from 10 to 200 nm. (e) Comparison of the temperature evolution of τ_{ANN} and τ_{flow} for PMPS in AAO nanopores of 100 nm in diameter. (f) Annealing time constant τ_{ANN} vs characteristic time of the viscous flow in cylindrical channels plotted on log-log scale for PMPS annealed at T = 258 K in different pore sizes. Evolution of both quantities in nanometer-size pores follow, with a very good approximation to each other ($s = 0.9$). Dashed lines represent linear fits to the data.

For the same quench depth (ΔT), the segmental relaxation time at the onset of the annealing deviates more from the bulk when lowering the temperature in 100 nm pores rather than reducing the pore size under isothermal conditions (T = 258 K).

Intuitively, the process equilibration in nanopore confinement—same as for bulk glasses aged below T_g—must be related to volume relaxation. However, the direct quantity that we follow in experiment is not the volume change as a function of time, but the segmental relaxation time which intrinsically depends on volume. On the way

towards an equilibrium, a glass former confined to nanometer pores loses the excess volume apparently gained or frozen at $T_{g\_\text{interface}}$ upon cooling, and tries to reach the level characteristic for the bulk liquid at the same temperature. In turn, as the molecular surroundings get more crowded, the segmental mobility slows down.

In Figs. 2(c) and 2(d) we have plotted the annealing time constant τ_{ANN}—obtained from the analysis of the kinetics of the equilibration process—vs ΔV, defined as the difference in the specific volume between bulk and confined material. For PMPS confined to AAO nanopores, V_{confined} refers to the initial value which becomes practically frozen on the experimental time scale at $T_{g\_\text{interface}}$ when doing cooling jumps with the rate of 5 K/ min. We obtain this value by knowing that τ_α follows the isochoric dependence below the vitrification temperature of the interfacial layer (see Fig. 1). The negative sign indicates the amount of surplus free volume that must be eliminated in order to regain the bulklike behavior. For both types of experimental approaches utilized to study the annealing kinetics in confinement, we observe a strong negative correlation between τ_{ANN} and ΔV. Thus, the larger the deviations from bulklike dynamics, (i.e., perturbation in volume in nanopore confinement) the longer the times needed to smooth it out.

To make this study more robust, we need to understand the mechanism which underlies such an equilibration process seen in 2D confinement. As the recovery of equilibrium in nanoconfinement requires much longer times than that corresponding to the α-relaxation time, we cannot simply assume that it is governed by the changes in the segmental mobility upon annealing. In search of the appropriate concept allowing us to describe the equilibrium recovery in nanopores, we have noted a striking similarity to the situation in which a liquid maintained inside a straight channel or a tube (made of a material having a much smaller thermal expansion coefficient) experiences cooling from room temperature down to around the glass-transition temperature. In a such case, a drop in temperature gives rise to an internal pressure in the liquid (also known as an energy-volume coefficient, $\Delta p = \Delta T \alpha_p \kappa^{-1}$) which is released via volume flow. At low temperatures, the ultraviscous liquid becomes immobilized and cannot flow in the channel. Instead, the liquid acts as if it were clamped to the surface of the walls. Similar reasoning was applied to thermal expansivity measurements of molecular glass formers or thin polymer films with the use of a capacitive method (parallel plate capacitor filled with a liquid which, by either volume contraction or expansion, controls the spacing between the plates) [45–47].

According to Poiseuilles law, the viscous flow rate in a cylindrical tube is proportional to the fourth power of the radius and inversely proportional to the liquid viscosity [48]. In other words, these two parameters critically impact on the time frames needed to eliminate volume or pressure effects close to T_g. For a bulk liquid, the characteristic flow time at T_g, where $\tau_\alpha = 100$ seconds, might take several days or more, depending on the geometry. In nanopore confinement, the viscous flow is even more strongly impeded. The characteristic viscous flow rate in uniform vertical nanochannels can be estimated as $\tau_{\text{flow}} \propto (l/r)^2 \tau_\alpha$ where l is the pore length (direction of the flow), r is the pore radius (direction perpendicular to the flow). Calculated values of τ_{flow} for PMPS confined within porous alumina channels of 100 μm in length and average pore diameter of 100 nm are presented together with τ_{ANN} in Fig. 2(e). It can be seen that both characteristic time constants have almost the same temperature dependence [49]. The results obtained when varying the pore diameter under isothermal conditions have led us to exactly the same finding. When the relationship between τ_{flow} and τ_{ANN} is analyzed using a log-log scale, it yields a straight line with the slope $s = 0.9$ [see Fig. 2(f)]. A value close to one signifies a coupling between both time scales, meaning that the annealing time constant tracks the ongoing changes in the viscous flow which must overcome the restriction imposed by nanoscale confinement. This evidence suggests that the faster dynamics of nanopore confined polymers is released through the extremely slow flux which eventually helps to eliminate surplus volume gained below $T_{g\_\text{interface}}$.

As the last point, we should realize the ability of a nanopore-confined system to maintain the recovered bulklike dynamics. Figure 3 demonstrates that PMPS confined

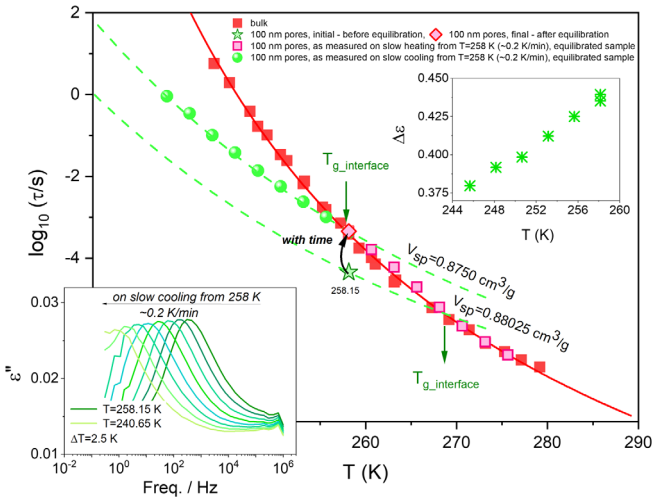

FIG. 3. Segmental (α-) relaxation time plotted vs temperature for PMPS in the bulk and confined to 100 nm AAO nanopores, as measured before and after annealing. Green star indicates α-relaxation time at the onset, while the pink diamond at the final stage of annealing carried out at T = 258 K. Pink squares represent evolution of $\tau_\alpha(T)$ dependence as measured on heating after equilibration at 258 K. The same type of experiment performed on cooling (green balls) results in deviation from the bulk VFT behavior and isochoric dependence. The lower inset shows dielectric loss spectra, while the upper inset changes in the dielectric strength that accompanies cooling from 258 K of the equilibrated nanoconfined polymer.

to 100 nm pores with the fully equilibrated mobility (as regained after prolonged annealing at 258 K) follows the same T dependences of the α-relaxation time on heating as in the bulk. On the other hand, cooling from 258 K down to a lower temperature drives it out of equilibrium once more. The story essentially starts all over again—$\tau_\alpha(T)$ departs from the bulklike behavior and follows an isochoric dependence. Annealing shifts $T_{g\_\text{interface}}$ towards lower temperatures and reduces the amount of free volume available for frustration in confinement. As the temperature decreases, the α relaxation loses its intensity (see insets in Fig. 3) because polymer chains located close to the pore walls again become immobilized via surface interactions.

In conclusion, we have demonstrated that confinement effects which lead to faster dynamics in nanopores have a very limited lifetime and diminish once enough time is provided to rearrange and attain a more densely packed alignment of the polymer chains. This is in line with the recent results reported for thin films. We found that the mechanism which governs the equilibration kinetics is related to exceedingly slow viscous flow in cylindrical channels of nanometer size. Hence, our finding might be proof that a correlation length is not at the origin of deviation from the VFT behavior. This work also provides new arguments that nanoscale and bulk glassy dynamics are connected, and by taking advantage of macroscopic studies of glass formers, we can still provide a satisfactory description of the origin of dramatic changes observed at the nanoscale level. Last, we expect that such nonequilibrium behavior of soft matter in confinement could be a more general feature that includes not only polymers, but also low-molecular-weight liquids.

K. A. acknowledge financial assistance from the National Science Centre (Poland) within Project OPUS 14 No. UMO-2017/27/B/ST3/00402. The authors also thank Kamil Kaminski for useful discussions and Ranko Richert for careful reading of the manuscript.

*kadrjano@us.edu.pl

[1] J. A. Forrest, K. Dalnoki-Veress, J. R. Stevens, and J. R. Dutcher, Phys. Rev. Lett. **77**, 2002 (1996).
[2] J.-Y. Park and G. B. McKenna, Phys. Rev. B **61**, 6667 (2000).
[3] M. Arndt, R. Stannarius, H. Groothues, E. Hempel, and F. Kremer, Phys. Rev. Lett. **79**, 2077 (1997).
[4] F. Kremer, A. Huwe, M. Arndt, P. Behrens, and W. Schwieger, J. Phys. Condens. Matter **11**, A175 (1999).
[5] R. Stannarius, F. Kremer, and M. Arndt, Phys. Rev. Lett. **75**, 4698 (1995).
[6] K. Adrjanowicz, K. Kolodziejczyk, W. K. Kipnusu, M. Tarnacka, E. U. Mapesa, E. Kaminska, S. Pawlus, K. Kaminski, and M. Paluch, J. Phys. Chem. C **119**, 14366 (2015).
[7] K. Adrjanowicz, K. Kaminski, K. Koperwas, and M. Paluch, Phys. Rev. Lett. **115**, 265702 (2015).
[8] K. Adrjanowicz, K. Kaminski, M. Tarnacka, G. Szklarz, and M. Paluch, J. Phys. Chem. Lett. **8**, 696 (2017).
[9] C. Zhang, Y. Sha, Y. Zhang, T. Cai, L. Li, D. Zhou, X. Wang, and G. Xue, J. Phys. Chem. B **121**, 10704 (2017).
[10] L. Li, D. Zhou, D. Huang, and G. Xue, Macromolecules **47**, 297 (2014).
[11] E. G. Merino, P. D. Neves, I. M. Fonseca, F. Danede, A. Idrissi, J. C. Dias, M. Dionsio, and N. T. Correia, J. Phys. Chem. C **117**, 21516 (2013).
[12] M. Tarnacka, K. Kaminski, E. Kaminska, C. M. Roland, and M. Paluch, J. Phys. Chem. C **120**, 7373 (2016).
[13] M. Tarnacka, K. Kaminski, E. U. Mapesa, E. Kaminska, and M. Paluch, Macromolecules **49**, 6678 (2016).
[14] M. Tarnacka, O. Madejczyk, K. Kaminski, and M. Paluch, Macromolecules **50**, 5188 (2017).
[15] X. Yan, C. Streck, and R. Richert, Ber. Bunsenges. Phys. Chem. **100**, 1392 (1996).
[16] I. M. Hodge, Science **267**, 1945 (1995).
[17] T. Hecksher, N. B. Olsen, K. Niss, and J. C. Dyre, J. Chem. Phys. **133**, 174514 (2010).
[18] D. Cangialosi, V. M. Boucher, A. Alegria, and J. Colmenero, Soft Matter **9**, 8619 (2013).
[19] R. D. Priestley, C. J. Ellison, L. J. Broadbelt, and J. M. Torkelson, Science **309**, 456 (2005).
[20] Y. Guo, C. Zhang, C. Lai, R. D. Priestley, M. D'Acunzi, and G. Fytas, ACS Nano **5**, 5365 (2011).
[21] S. Simon, J.-Y. Park, and G. McKenna, Eur. Phys. J. E **8**, 209 (2002).
[22] S. Napolitano and M. Wübbenhorst, Nat. Commun. **2**, 260 (2011).
[23] N. G. Perez-de-Eulate, M. Sferrazza, D. Cangialosi, and S. Napolitano, ACS Macro Lett. **6**, 354 (2017).
[24] A. Panagopoulou and S. Napolitano, Phys. Rev. Lett. **119**, 097801 (2017).
[25] M. Paluch, S. Pawlus, and C. M. Roland, Macromolecules **35**, 7338 (2002).
[26] M. Paluch, R. Casalini, A. Patkowski, T. Pakula, and C. M. Roland, Phys. Rev. E **68**, 031802 (2003).
[27] M. Paluch, C. M. Roland, and S. Pawlus, J. Chem. Phys. **116**, 10932 (2002).
[28] S. Pawlus, S. J. Rzoska, J. Ziolo, M. Paluch, and C. M. Roland, Rubber Chem. Technol. **76**, 1106 (2003).
[29] W. K. Kipnusu, M. Elsayed, R. Krause-Rehberg, and F. Kremer, J. Chem. Phys. **146**, 203302 (2017).
[30] A. Schönhals, H. Goering, Ch. Schick, B. Frick, and R. Zorn, J. Non-Cryst. Solids **351**, 2668 (2005).
[31] A. Schönhals, R. Zorn, and B. Frick, Polymer **105**, 393 (2016).
[32] K. Chrissopoulou, S. H. Anastasiadis, E. P. Gianneli, and B. Frick, Polymer **127**, 144910 (2007).
[33] S. Alexandris, P. Papadopoulos, G. Sakellariou, M. Steinhart, H.-J. Butt, and G. Floudas, Macromolecules **49**, 7400 (2016).
[34] Z. Zhou and D. Yan, Macromol. Theory Simul. **6**, 579 (1997).
[35] M. Graca, S. A. Wieczorek, M. Fijalkowski, and R. Holyst, Macromolecules **35**, 9117 (2002).
[36] See Supplemental Material at http://link.aps.org/supplemental/10.1103/PhysRevLett.122.176101 for further details on materials and methods, sample preparation, data

treatment, additional results demonstrating the effect of various thermal protocol on $\tau_\alpha(T)$ dependence measured in nanopores, information on how to determine isochoric dependences of the α-relaxation time in confinement, analysis of the equilibration kinetics with the use of stretched exponential function, calorimetric results, and evolution of τ_α upon isothermal annealing of PMPS in AAO nanopores of different pore sizes, which includes Refs. [37,38].

[37] D. Boese, B. Momper, G. Meier, F. Kremer, J.-U. Hagenah, and E. W. Fischer, Macromolecules **22**, 4416 (1989).

[38] L. Li, J. Chen, W. Deng, C. Zhang, Y. Sha, Z. Cheng, G. Xue, and D. Zhou, J. Phys. Chem. B **119**, 5047 (2015).

[39] J. H. Dymond and R. Malhotra, Int. J. Thermophys. **9**, 941 (1998).

[40] R. Casalini, U. Mohanty, and C. M. Roland, Chem. Phys. **125**, 014505 (2006).

[41] R. P. White and J. E. G Lipson, Macromolecules **49**, 3987 (2016).

[42] W. K. Kipnusu, M. Elsayed, W. Kossack, S. Pawlus, K. Adrjanowicz, M. Tress, E. U. Mapesa, R. Krause-Rehberg, K. Kaminski, and F. Kremer, J. Phys. Chem. Lett. **6**, 3708 (2015).

[43] J.-Y. Park and G. B. McKenna, Condens. Matter Mater. Phys. **61**, 6667 (2000).

[44] G. Szklarz, K. Adrjanowicz, M. Tarnacka, J. Pionteck, and M. Paluch, J. Phys. Chem. C **122**, 1384 (2018).

[45] C. Bauer, R. Richert, R. Bohmer, and T. Christensen, J. Non-Cryst. Solids **262**, 276 (2000).

[46] C. Bauer, R. Bohmer, S. Moreno-Flores, R. Richert, H. Sillescu, and D. Neher, Phys. Rev. E **61**, 1755 (2000).

[47] K. Niss, D. Gundermann, T. Christensen, and J. C. Dyre, Phys. Rev. E **85**, 041501 (2012).

[48] B. Lautrup, *Physics of Continuous Matter* (IOP, Bristol, 2005).

[49] Here, we made a number of crude estimations like the fluid inside the pores having spatially uniform properties, only the pressure gradient drives the flow, while viscosity balances it. We also do not take into account the strain relaxation perpendicular to the pore axis or the impact of the surface interactions. Nevertheless, obtained results and the idea of considering viscous flow effects to explain equilibration behavior of nanopore-confined glass formers provide some elementary understanding of the phenomena observed in nanometer size channels and constitute a good starting point for more complicated theoretical studies in the future.